

EUROPHYSICS LETTERS

*Europhys. Lett.*, (), pp. ()

## Residual Symmetries in the Spectrum of Periodically Driven Alkali Rydberg States

ANDREAS KRUG<sup>1,2,3</sup> AND ANDREAS BUCHLEITNER<sup>1,3</sup>

<sup>1</sup> *Max-Planck-Institut für Physik komplexer Systeme, Nöthnitzer-Str. 38, D-01069 Dresden;* <sup>2</sup> *Max-Planck-Institut für Quantenoptik, Hans-Kopfermann-Str. 1, D-85748 Garching b. München;* <sup>3</sup> *Sektion Physik der Ludwig-Maximilians-Universität München, Schellingstr. 4, D-80799 München.*

(received ; accepted )

PACS. 32.80Rm – Multiphoton ionization and excitation to highly excited states (e.g., Rydberg states).

PACS. 05.45+b – Theory and models of chaotic systems.

PACS. 42.50Hz – Strong-field excitation of optical transitions in quantum systems; multiphoton processes; dynamic Stark shift.

**Abstract.** – We identify a fundamental structure in the spectrum of microwave driven alkali Rydberg states, which highlights the remnants of the Coulomb symmetry in the presence of a non-hydrogenic core. Core-induced corrections with respect to the hydrogen spectrum can be accounted for by a perturbative approach.

*Introduction.* – The excitation and subsequent ionization of Rydberg states of atomic hydrogen by microwave fields is one of the most prominent examples of the manifestation of classically nonlinear dynamics in a realistic physical system [1]. Given a driving field frequency comparable to the classical Kepler frequency of the unperturbed Rydberg electron, the electron's classical trajectory goes chaotic for sufficiently large driving field amplitudes, finally leading to its ionization on a finite time scale [2]. Correspondingly, large ionization rates are observed in experiments on real (i.e., quantum) Rydberg states of atomic hydrogen, in the appropriate parameter range [1, 3].

As a matter of fact, already before the onset of classically chaotic motion, i.e. at not too large driving field amplitudes, individual quantum eigenstates of the atom in the field exhibit energies and ionization rates which are determined only by the orbital parameters of the classical trajectory they are associated with [4]. Those orbits which are the least stable under the external perturbation (i.e., which turn chaotic for the lowest values of the driving field amplitude, such as straight line orbits parallel to the field polarization axis for a linearly polarized drive) induce the largest ionization rates for their associated eigenstates. Consequently, in this near-integrable regime of classical dynamics, it is possible to classify the eigenstates of the atom in the field through quantum numbers associated with the orbital parameters of unperturbed Kepler ellipses, i.e. with the angular momentum and the Runge-

Lenz vector. An adiabatic invariant governs the slow evolution of these parameters under external driving [4].

It should be noted, however, that a considerable part of experimental data has been accumulated in experiments on Rydberg states of alkali atoms rather than of atomic hydrogen [5, 6, 7, 8, 9, 10]. A priori, a classical-quantum correspondence as briefly sketched above for atomic hydrogen cannot be established here, due to the absence of a well and uniquely defined classical Hamiltonian. In particular, the atomic core destroys the symmetry characteristic for the hydrogen atom and the Runge-Lenz vector is no more a constant of motion.

Indeed, experimental data systematically suggest strongly enhanced ionization rates of nonhydrogenic (i.e., low angular momentum) alkali Rydberg states as compared to atomic hydrogen [5, 6, 7, 9, 10], though they also exhibit qualitatively similar features, e.g. of the dependence of the ionization yield on the principal quantum number of the atomic state the atoms are initially prepared in [9, 10]. On the other hand, a direct comparison of available hydrogen and alkali data is somewhat questionable, since relevant experimental parameters such as the interaction time of the atom with the field are typically different for different experiments. Furthermore, a rigorous theoretical treatment of alkali atoms exposed to microwave fields was not accomplished until now.

It is the purpose of the present letter to outline such a rigorous treatment which allows for the first time for a *direct* comparison of hydrogen and alkali ionization dynamics under *precisely the same* conditions, without adjustable parameters. First results of our numerical experiments directly address the above question of quantum-classical correspondence for periodically driven alkali atoms.

*Theory.* – Let us start with the nonrelativistic Hamiltonian of a one-electron atom exposed to a linearly polarized microwave field of (constant) amplitude  $F$  and frequency  $\omega$ , in length gauge, employing the dipole approximation and atomic units:

$$H(t) = \frac{\mathbf{p}^2}{2} + V_{\text{atom}}(r) + Fz \cos \omega t, \quad r > 0. \quad (1)$$

As this Hamiltonian is periodic in time, we can use the Floquet theorem [11] to find the eigenstates (“dressed states”) of the atom in the field. After integration over the solid angle we have to solve the time-independent, radial eigenvalue equation

$$\begin{aligned} & \left( -\frac{d^2}{dr^2} + \frac{\ell(\ell+1)}{r^2} + 2V_{\text{atom}}(r) - 2k\omega - 2\varepsilon \right) |\Psi_{\varepsilon, \ell}^k\rangle \\ & + FrA_{\ell+1} \left( |\Psi_{\varepsilon, \ell+1}^{k-1}\rangle + |\Psi_{\varepsilon, \ell+1}^{k+1}\rangle \right) + FrA_{\ell} \left( |\Psi_{\varepsilon, \ell-1}^{k-1}\rangle + |\Psi_{\varepsilon, \ell-1}^{k+1}\rangle \right) = 0, \\ & \text{with } A_{\ell} = \sqrt{\frac{\ell^2 - m^2}{4\ell^2 - 1}}; \quad \ell = 0, 1, 2, \dots; \quad k = -\infty, \dots, +\infty. \end{aligned} \quad (2)$$

The additional quantum number  $k$  counts the number of photons that are exchanged between the atom and the field, and  $\varepsilon$  denotes the quasi-energy of the dressed state

$$|\Psi_{\varepsilon}\rangle = \sum_k \exp(-ik\omega t) |\Psi_{\varepsilon}^k\rangle = \sum_{k, \ell} \exp(-ik\omega t) Y_{\ell, m}(\theta, \phi) |\Psi_{\varepsilon, \ell}^k\rangle / r, \quad (3)$$

with  $Y_{\ell, m}(\theta, \phi)$  the spherical harmonics.  $m$  denotes the angular momentum projection on the field polarization axis and remains a good quantum number, due to the rotational symmetry of our problem around the field axis. For all numerical results presented hereafter, its value was fixed to  $m = 0$ . As immediately obvious from the nondiagonal part of eq. (2), the interaction with the linearly polarised microwave field conserves the generalised parity  $\Pi = (-1)^{k+\ell}$ . This

just expresses the angular momentum transfer associated with the absorption (emission) of a photon.

As a unique one-particle potential  $V_{\text{atom}}(r)$  for alkali atoms is unknown, we use a variant [12] of R-matrix theory to describe the interaction of the outer electron with the atomic core. Configuration space is divided in two regions: In the internal region,  $0 < r \leq a$ , the external field is negligible compared to the field created by the atomic core, and the details of the interaction are unknown. With the help of quantum defect theory [13], the solution of eq. (2) at  $r = a$  can be written as a linear combination of regular and irregular Coulomb-functions  $s_{\ell,E}(r)$  and  $c_{\ell,E}(r)$ ,

$$F_{\ell,E}(r) = \cos(\pi\delta_{\ell})s_{\ell,E}(r) + \sin(\pi\delta_{\ell})c_{\ell,E}(r), \quad r = a, \quad (4)$$

where the  $\delta_{\ell}$  are the quantum defects [13] known from spectroscopic experimental data [14]. In the outer region,  $r > a$ , the difference between the actual atomic potential  $V_{\text{atom}}(r)$  and the Coulomb potential  $-1/r$  can be neglected. However, the operator  $d^2/dr^2$  is no more hermitian in the reduced range  $a < r < \infty$ . To overcome this problem, a surface term  $\delta(r-a)(\frac{\partial}{\partial r} + C_{\ell})$  is added [12, 16] to the diagonal part of (2). The matching condition between inner and outer region at  $r = a$  is incorporated in the constant  $C_{\ell}$  by defining

$$C_{\ell} = (F_{\ell,\varepsilon+k\omega}(r))^{(-1)} \frac{\partial}{\partial r} F_{\ell,\varepsilon+k\omega}(r). \quad (5)$$

Note that the function  $F_{\ell,E}(r)$  in eq. (4) has to be evaluated at the energy  $\varepsilon + k\omega$  in (5), i.e. at different energies for different photon indices  $k$ . This generalizes the approach outlined in [12] to periodically driven systems.

Finally, due to the continuum coupling induced by the external field, all atomic bound states turn into resonances with finite ionization rates  $\Gamma_{\varepsilon}$ . In order to extract the latter together with the energies  $\varepsilon$  of the atom in the field, we use the method of complex scaling [15, 17]. After this nonunitary transformation the Floquet Hamiltonian amended by the core induced surface term (5) is represented by a complex symmetric matrix, with complex eigenvalues  $\varepsilon - i\Gamma_{\varepsilon}/2$ . These are obtained by diagonalization of the complex eigenvalue problem in a real Sturmian basis, using an efficient implementation of the Lanczos algorithm. Together with the associated eigenvectors they provide a complete description of our problem [15].

*Results.* – The described theoretical/numerical apparatus is now applied to alkali atoms in a microwave field. Since we want to identify the core induced effects in the alkali problem as compared to the hydrogen spectrum, we use parameter values which have been employed in earlier work on microwave driven Rydberg states [4, 15] of hydrogen. To keep the comparison as transparent as possible, we focus on a microwave frequency  $\omega = 1.07171794 \times 10^{-4}$  a.u. which is nonresonant with the hydrogen level spacing in the vicinity of the atomic initial state with principal quantum number  $n_0 = 23$ . The field amplitude is fixed to  $F = 1.072 \times 10^{-7}$  a.u., slightly below the onset of appreciable (chaos-induced [2]) ionization of atomic hydrogen [4]. This choice of parameters defines a near-integrable phase space structure for the classical dynamics of driven hydrogen, with an unambiguous signature in the associated quantum energies emerging from the  $n_0 = 23$  manifold. The black dots in fig. 1 illustrate the situation: The driving field lifts the angular momentum degeneracy of the substates of the manifold, which reorganize according to their localization properties in classical phase space [4]. Those states with maximum angular momentum and spherical symmetry experience the strongest field induced (“ac-”) shift in energy, whereas those with maximum radial component of the Runge-Lenz vector and “ $\lambda$ -symmetry” [4, 18, 19] remain essentially unaffected by the external perturbation. Since the low angular momentum states are strongly mixed by the field (to

build states with  $\lambda$ -symmetry [18, 19]), a new (semiclassical) quantum number  $p$  [4] is used to label the  $n_0$  substates of the manifold in the field.  $p$  is an integer ranging from 0 to  $n_0 - 1$ , and simply counts the number of quanta enclosed by a semiclassical contour integral along the equipotential curves of the adiabatic Hamiltonian which generates the slow evolution of angular momentum and Runge-Lenz vector of the classical Kepler ellipse under external driving [4]. The associated eigenstates exhibit spherical symmetry for  $p = 0 \dots 9$ , and  $\lambda$ -symmetry for  $p = 10 \dots 22$ , respectively [4]. Note that low and high  $p$ -values correspond to negligible ionization rates of the atom in the field, due to the *classical* stability of the associated trajectories under external driving [4]. Actually, the  $\lambda$ -states with large  $p$ , which quantize a classical straight line orbit perpendicular to the field polarization axis, with maximum modulus of the Runge-Lenz vector, display the smallest ionization rates [4].

In the presence of a non-hydrogenic core, the Runge-Lenz vector is no more a conserved quantity and the  $\lambda$ -symmetry defining associated eigenstates of the field free atom [18] is destroyed. Therefore, no symmetry argument is available to predict a similar (semiclassical) organization of the alkali energy levels under external driving, alike the one observed for atomic hydrogen [4].

Nonwithstanding, our results for lithium Rydberg states exposed to precisely the same external perturbation as for the hydrogen results clearly show that the symmetry properties of the driven Coulomb problem prevail even in the presence of the core. As evident from the open triangles in fig. 1 (a), the hydrogenic part of the lithium manifold exhibits globally the same (semiclassical) structure as the hydrogen levels. For low values of  $p$  ( $\simeq 0 \dots 9$ ) this is not surprising as the associated classical trajectories (large angular momenta) do not probe the atomic core [4]. However, for large  $p$ -values ( $\simeq 10 \dots 20$ ), the classical solution of the Coulomb problem does impinge on the nucleus and will certainly suffer scattering off the nonhydrogenic core. Yet, in the presence of the field, this scattering obviously mixes states of  $\lambda$  type only and does not affect the overall separation of the spectrum in spherical and  $\lambda$  states, as a remnant of the classical phase space structure of the driven Coulomb dynamics. Neither does the presence of the core appreciably affect the ionization rates of the dressed states, as obvious from fig. 1 (b). Only at  $p = 10$  is there a local enhancement of the width (by approx. one order of magnitude), due to the near resonant coupling of the state to the nonhydrogenic eigenstate originating from  $|n = 41, \ell = 0\rangle$ , via a six-photon transition (similarly, a very weak multiphoton coupling slightly enhances the width of the  $p = 12$  state). In the near integrable regime of the classical Coulomb dynamics we are considering here it is precisely this kind of multiphoton resonances between nonhydrogenic (low  $\ell$ , such that  $\delta_\ell \neq 0$ ) states and hydrogenic manifolds which provides a channel for enhanced ionization as compared to atomic hydrogen. Note that without such a near resonant coupling, the non-hydrogenic states of a given manifold tend to be *more* stable than the hydrogenic ones, as they are highly isolated in the spectrum. As an example, for the same field parameters, the lithium  $n_0 = 23$   $\ell = 0$  ( $\delta_{\ell=0} = 0.399468$ ) and  $\ell = 1$  ( $\delta_{\ell=1} = 0.047263$ ) [14] states exhibit ionization rates  $\Gamma_\varepsilon \sim 10^{-15}$  a.u. as small as the most stable substates of the hydrogenic manifold of fig. 1. A detailed analysis of enhanced ionization via core-induced multiphoton resonances will be provided elsewhere.

Closer inspection of fig. 1 (a) shows additional structure in the alkali spectrum, on top of the globally hydrogen-like structure: for large values of  $p$  ( $\geq 11$ ), the alkali levels are shifted with respect to the hydrogenic energies. These shifts can be recovered by diagonalization of the hydrogen problem within the restricted subspace spanned by the hydrogenic levels of the alkali Rydberg manifold [19, 20, 21, 22]. In other words, the shifted energies are the solutions of the eigenvalue equation

$$PH_{\text{hyd}}P|\Phi^{k_0}\rangle = (E + k_0\omega)|\Phi^{k_0}\rangle, \quad (6)$$

where  $H_{\text{hyd}}$  is obtained from (1) setting  $V_{\text{atom}}(r) = -1/r$ ,  $r \in ]0, \infty[$ , and  $P$  the projector onto the hydrogenic subspace of the alkali manifold labeled by the principal quantum number  $n_0$  and the photon number  $k_0$ . Such a procedure is legitimate as long as the states emerging from the nonhydrogenic part of the alkali manifold have vanishing overlap with the complete hydrogen manifold emanating from  $(n_0, k_0)$ . This condition is fulfilled for the driving field strength considered here.

Solving (6) for  $E$  is tantamount to finding the roots of

$$\det(Q \frac{1}{H_{\text{hyd}} - (E + k_0\omega)} Q) = 0, \quad (7)$$

with  $Q = 1 - P$  the projector onto the orthogonal complement of the hydrogenic subspace for given  $(n_0, k_0)$ . Without loss of generality we choose  $k_0 = 0$  hereafter. Consequently, for one single non-vanishing quantum defect  $\delta_{\ell_0}$ , (7) becomes

$$\sum_{\varepsilon} \frac{|\langle n_0, \ell_0 | \Psi_{\varepsilon}^{k_0=0} \rangle|^2}{\varepsilon - E} = 0, \quad (8)$$

where  $|n_0, \ell_0\rangle$  spans the orthogonal complement of the hydrogenic subspace of the alkali atom within the  $(n_0, k_0 = 0)$  manifold. Note that (7) or (8) have to be evaluated for different values of the generalized parity  $\Pi$ , and that we have to solve (8) separately for  $\ell_0 = 0$  and  $\ell_0 = 1$ , in order to recover the level shifts observed for lithium in fig. 1 (the  $\ell_0 = 2$  and  $\ell_0 = 3$  states of lithium remain within the range of  $P$ , due to their negligible quantum defects  $\delta_{\ell=2} = 0.002129$  and  $\delta_{\ell=2} = -0.000077$  [14], at the given field strength). Fig. 2 (a) shows the result of the projection method, compared to the exact numerical result – the agreement is very good. Since the low  $p$  states essentially exhibit spherical symmetry with large angular momentum projection, their overlap with  $|n_0, \ell_0 = 0(\ell_0 = 1)\rangle$  vanishes and their energies remain unshifted as compared to the hydrogen results.

The scenario which we described for lithium also applies for the heavier alkali elements, as illustrated in figs. 2 (b) and (c). Here we plot the shifts of the exact energies of sodium and rubidium with respect to the hydrogen levels, as they emerge from the  $n_0 = 23$  manifold, for precisely the same field parameters as used for the lithium results. Since for these elements also the  $\ell_1 = 2$  (sodium) and the  $\ell_1 = 3$  (rubidium) states are separated from the hydrogenic manifold due to their large quantum defects, the range of  $Q$  in (7) is two-dimensional and the evaluation of the determinant yields the expression

$$\sum_{\varepsilon} \frac{|\langle n_0, \ell_0 | \Psi_{\varepsilon}^{k_0=0} \rangle|^2}{\varepsilon - E} \sum_{\varepsilon} \frac{|\langle n_0, \ell_1 | \Psi_{\varepsilon}^{k_0=0} \rangle|^2}{\varepsilon - E} - \left[ \sum_{\varepsilon} \frac{\langle n_0, \ell_0 | \Psi_{\varepsilon}^{k_0=0} \rangle \langle \Psi_{\varepsilon}^{k_0=0} | n_0, \ell_1 \rangle}{\varepsilon - E} \right]^2 = 0. \quad (9)$$

Again, the solution of (9) gives very good agreement with the numerical result. In addition, we note that the larger the dimension of the range of  $Q$ , the smaller the values of  $p$  for which the alkali levels are shifted as compared to the hydrogen energies. This is a consequence of the dominance of small  $\ell$  components in large  $p$  states and of large  $\ell$  components in small  $p$  states, since the heavier the element the larger the  $\ell$  values affected by non-negligible quantum defects.

*Summary.* – In conclusion, the energy levels of alkali Rydberg states emerging from the hydrogenic  $n_0$ -manifold clearly reflect the phase space structure of the microwave driven Coulomb problem, despite the presence of a symmetry breaking atomic core. Also the ionization rates of the atoms reflect the underlying classical phase space structure, with the exception of local enhancements due to multiphoton resonances with nonhydrogenic sublevels of other manifolds.

We have checked that the observed structure is robust under changes of the driving field amplitude, up to values where adjacent  $n$ -manifolds start to overlap.

\*\*\*

We thank Dominique Delande and Ken Taylor for fruitful discussions and an introduction to the R-matrix approach of [12].

#### REFERENCES

- [1] KOCH P. M., *Physica D*, **83** (1995) 178.
- [2] CASATI G. *et al.*, *Phys. Rep.*, **154** (1987) 77.
- [3] BAYFIELD J. E. and KOCH P. M., *Phys. Rev. Lett.*, **33** (1974) 258.
- [4] BUCHLEITNER A. and DELANDE D., *Phys. Rev. A*, **55** (1997) R1585.
- [5] PILLET P. *et al.*, *Phys. Rev. A*, **30** (1984) 280.
- [6] GALLAGHER T. F. *et al.*, *Phys. Rev. A*, **39** (1989) 4545.
- [7] PANMING FU *et al.*, *Phys. Rev. Lett.*, **64** (1990) 511.
- [8] BLÜMEL *et al.*, *Phys. Rev.*, **44** (1991) 4521.
- [9] ARNDT M. *et al.*, *Phys. Rev. Lett.*, **67** (1991) 2435.
- [10] BENSON O. *et al.*, *Phys. Rev. A*, **51** (1995) 4862.
- [11] SHIRLEY J. H., *Phys. Rev.*, **138** (1965) B979.
- [12] HALLEY M. H. *et al.*, *J. Phys. B*, **26** (1993) 1775.
- [13] SEATON M. J., *Rep. Prog. Phys.*, **46** (1983) 167.
- [14] LORENZEN C.-J. and NIEMAX K., *Physica Scripta*, **27** (1983) 300.
- [15] BUCHLEITNER A. *et al.*, *J. Opt. Am. B*, **12** (1995) 505.
- [16] BLOCH C., *Nucl. Phys.*, **4** (1951) 5.
- [17] BALSLEV E. and COMBES J. M., *Commun. Math. Phys.*, **22** (1971) 280.
- [18] DELANDE D. and GAY J. C., *J. Phys. B*, **17** (1984) 335.
- [19] DELANDE D., *Thèse d'Etat*, Université Pierre et Marie Curie, Paris 1988 .
- [20] FABRE C. *et al.*, *J. Phys. B*, **17** (1984) 3217.
- [21] BRAUN P. A., *J. Phys. B*, **18** (1985) 4187.
- [22] PENENT F. *et al.*, *Phys. Rev. A*, **15** (1988) 4707.

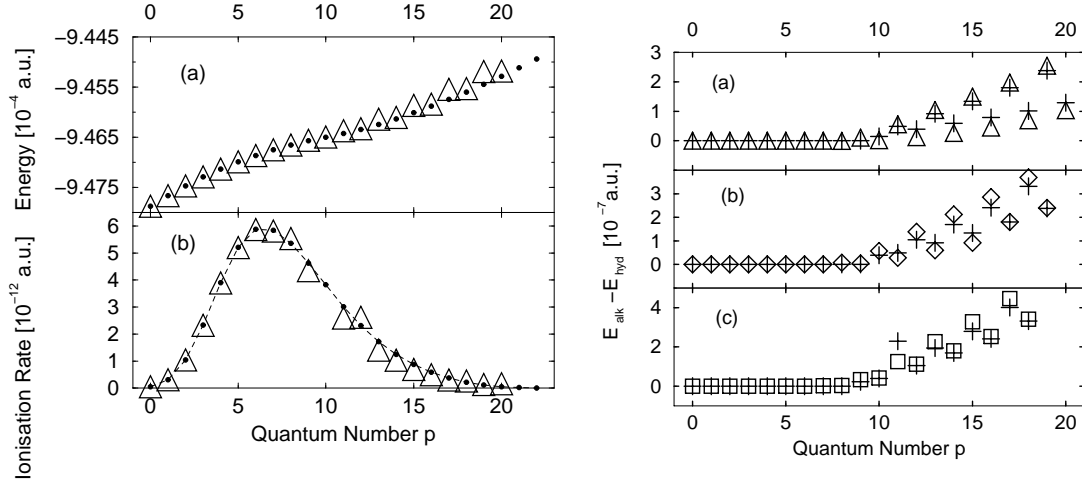


Fig. 1. – Energies (a) and ionisation rates (b) of Rydberg states of lithium (triangles) and of atomic hydrogen (dots) exposed to a linearly polarized microwave field of frequency  $\omega = 1.07171794 \times 10^{-4}$  a.u. and amplitude  $F = 1.072 \times 10^{-7}$  a.u., for principal quantum number  $n_0 = 23$  and angular momentum projection  $m = 0$  on the field polarization axis. The lithium spectrum lacks two of the 23 substates of the manifold, due to the quantum defects  $\delta_{\ell=0} = 0.399468$  and  $\delta_{\ell=1} = 0.047263$  of the  $\ell = 0$  and  $\ell = 1$  states, respectively. The quantum defects  $\delta_{\ell=2} = 0.002129$  and  $\delta_{\ell=3} = -0.000077$  are negligible compared to the field induced splitting of the  $n_0 = 23$  manifold (field-free energy  $E_{23} \simeq -9.452 \times 10^{-4}$  a.u.). Both spectra almost coincide (in energy and ionisation rate) even for larger values ( $p \geq 10$ ) of the (semiclassical [4]) quantum number  $p$ , despite the fact that the localization properties of the associated eigenstates (close to the plane defined by the field polarization axis) originate in the dynamical symmetry of the  $-1/r$  Coulomb potential [18]. The latter is *destroyed* by the presence of a nonhydrogenic core in alkali atoms. The ionization rate of the  $p = 10$  state of lithium is locally enhanced by approx. one order of magnitude with respect to the corresponding hydrogen eigenstate, due to a six-photon resonance with the  $|n = 41, \ell = 0\rangle$  state.

Fig. 2. – Shifts  $E_{\text{alk}} - E_{\text{hyd}}$  of the energies  $E_{\text{alk}}$  of lithium (a, triangles), sodium (b, diamonds), and rubidium (c, squares) as compared to those,  $E_{\text{hyd}}$ , of the  $n_0 = 23$  manifold of atomic hydrogen in a linearly polarized microwave field, with the same parameters as in fig. 1. Quantum defects employed for the sodium results:  $\delta_{\ell=0} = 1.347964$ ,  $\delta_{\ell=1} = 0.85538$ ,  $\delta_{\ell=2} = 0.015543$ ,  $\delta_{\ell=3} = 0.001453$ , and for rubidium:  $\delta_{\ell=0} = 3.1311$ ,  $\delta_{\ell=1} = 2.6415$ ,  $\delta_{\ell=2} = 1.3472$ ,  $\delta_{\ell=3} = 0.016312$  [14]. Consequently, three respectively four energy levels are missing in (b) and (c). The nonvanishing shifts for large  $p \geq 9$  values can be accounted for by projecting out the low  $\ell$  components (i.e. the ones with core induced energy shifts large with respect to the field induced splitting of the  $n_0 = 23$  manifold) of the  $n_0$ -manifold, as indicated by the crosses, see eqs. (8) and (9). The agreement between this perturbative approach and the exact quantum results is always better than the average level spacing of the hydrogen manifold (dots in fig. 1), except for the relatively large discrepancy at  $p = 11$ , in (c). The latter is due to a multiphoton resonance between the alkali eigenstate and a nonhydrogenic (low  $\ell$ ) state.